New nitrosyl ruthenium complexes with combined activities for multiple cardiovascular disorders

Florêncio Sousa Gouveia Júnior[a], João Alison de Moraes Silveira[b,c], Thais Muratori Holanda[b,c], Aline Diogo Marinho[c], Lisa A. Ridnour[d], David A. Wink[d], Rodrigo José Bezerra de Siqueira[b], Helena Serra Azul Monteiro[b,c], Eduardo Henrique Silva de Sousa[a*], Luiz Gonzaga de França Lopes[a*]

[a] Laboratory of Bioinorganic Chemistry, Department of Organic and Inorganic Chemistry, Federal University of Ceara, 60455-760, Fortaleza-CE, Brazil

[b]Department of Physiology and Pharmacology, School of Medicine, Federal University of Ceara, Coronel Nunes de Melo St., 1127, 60.430-275, Fortaleza-CE, Brazil.

[c]Drug Research and Development Center (NPDM), Federal University of Ceara, Coronel Nunes de Melo St., 1000, 60.430-275, Fortaleza-CE, Brazil

[d] National Cancer Institute, Cancer and Inflammation Program, Frederick, Maryland 21702, United States

*corresponding authors: eduardohss@dqoi.ufc.br; lopeslu@dqoi.ufc.br

Figure S1. Molecular structure representation of Sodium Nitroprusside (SNP) complex

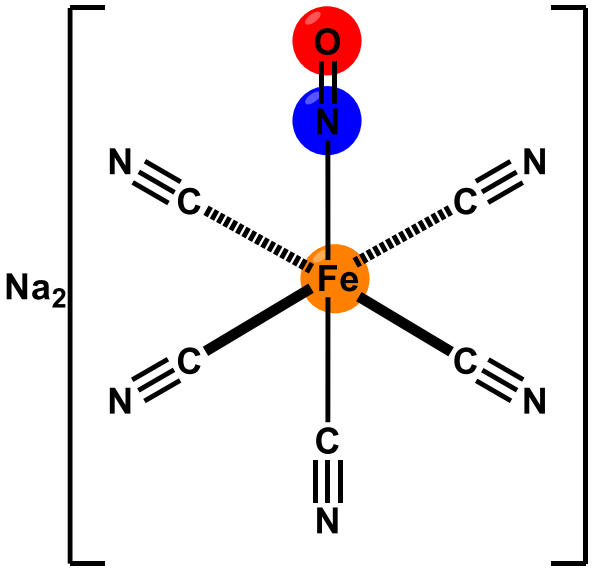

Figure S2. NMR spectra for complexes **Ru1-5**.

A) ^{1}H and COSY spectra for **Ru1**

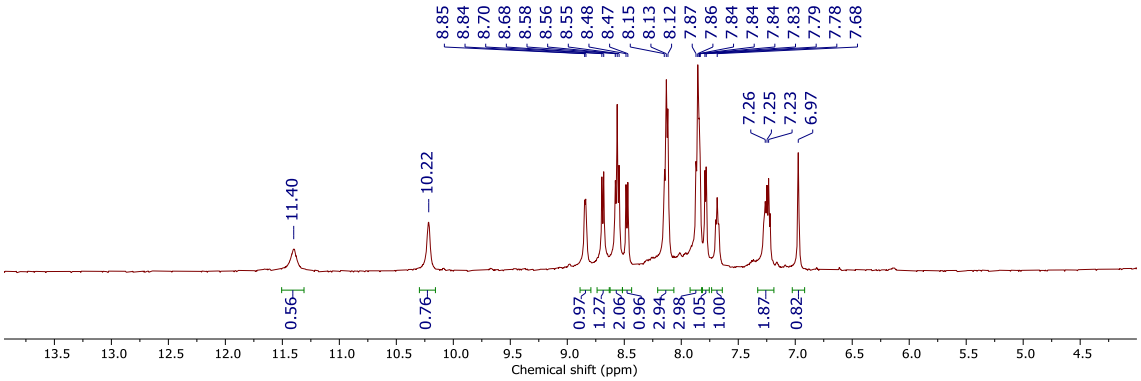

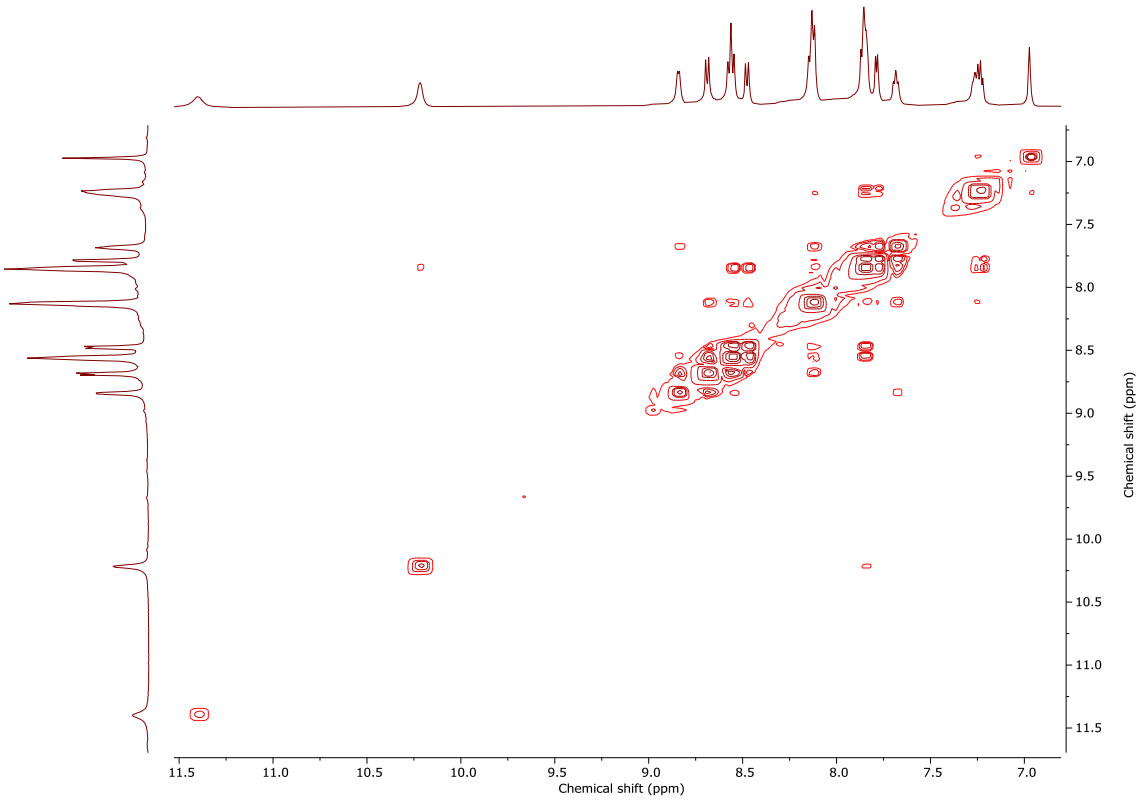

B) ^{1}H and COSY spectra for **Ru2**

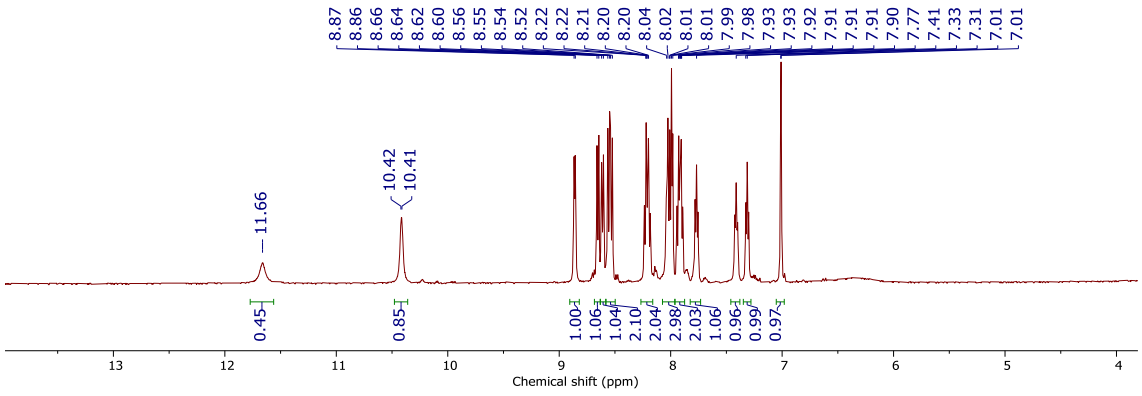

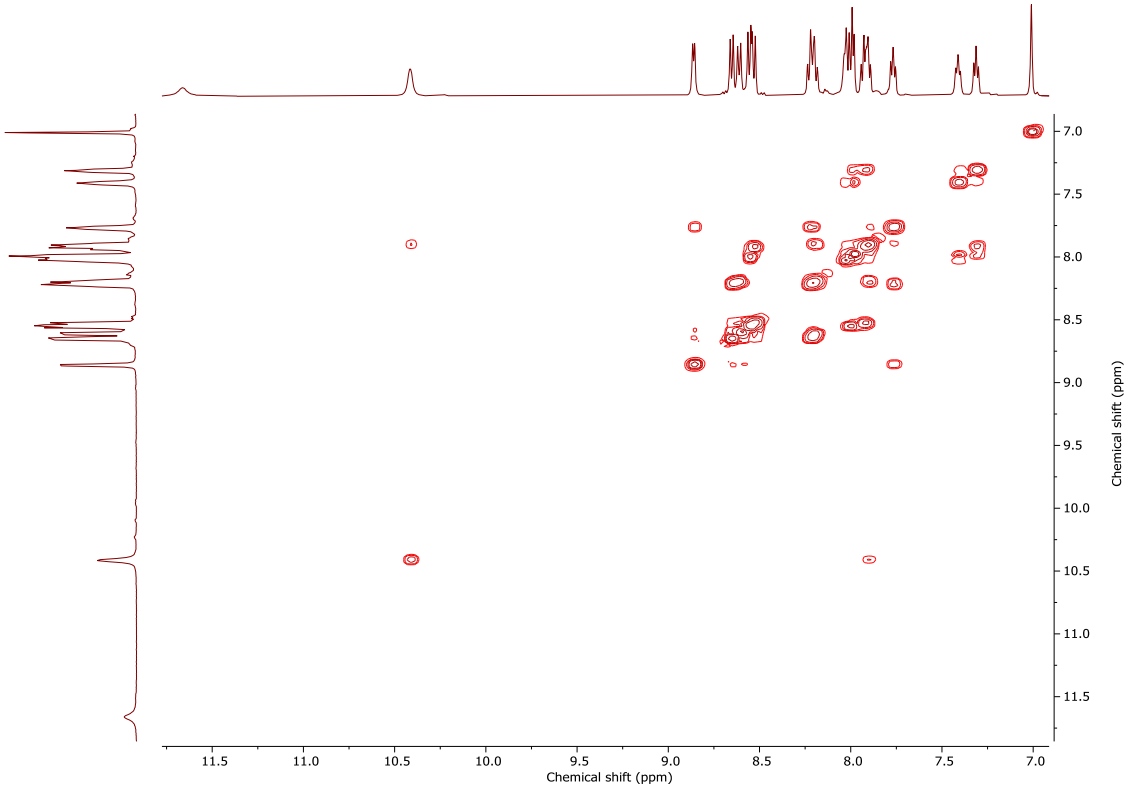

C) ^{1}H and COSY spectra for **Ru3**

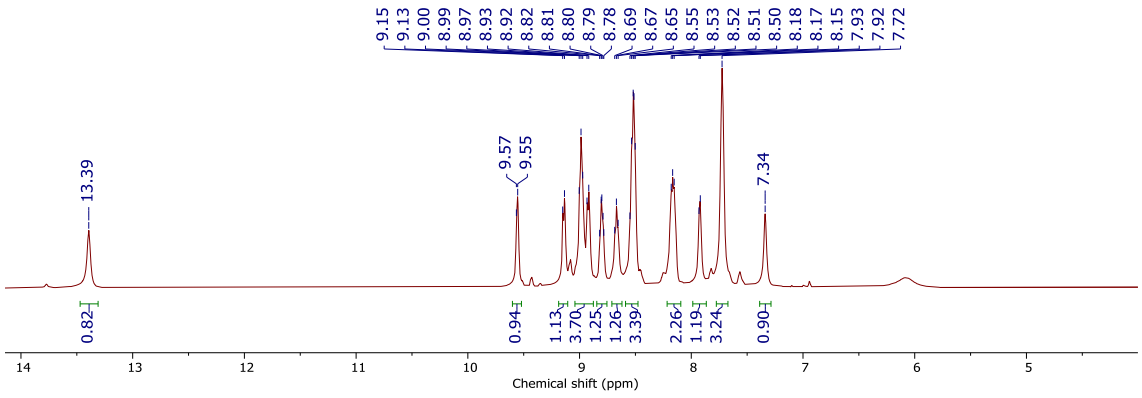

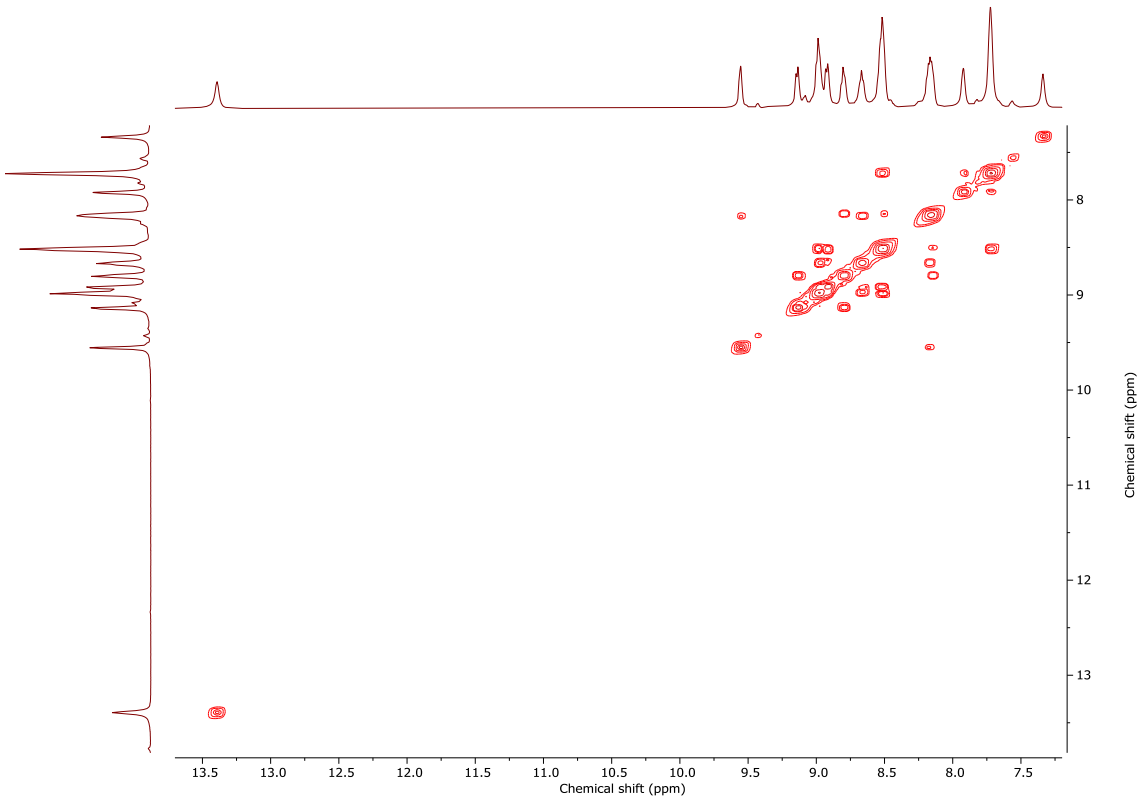

D) ^{1}H and COSY spectra for **Ru4**

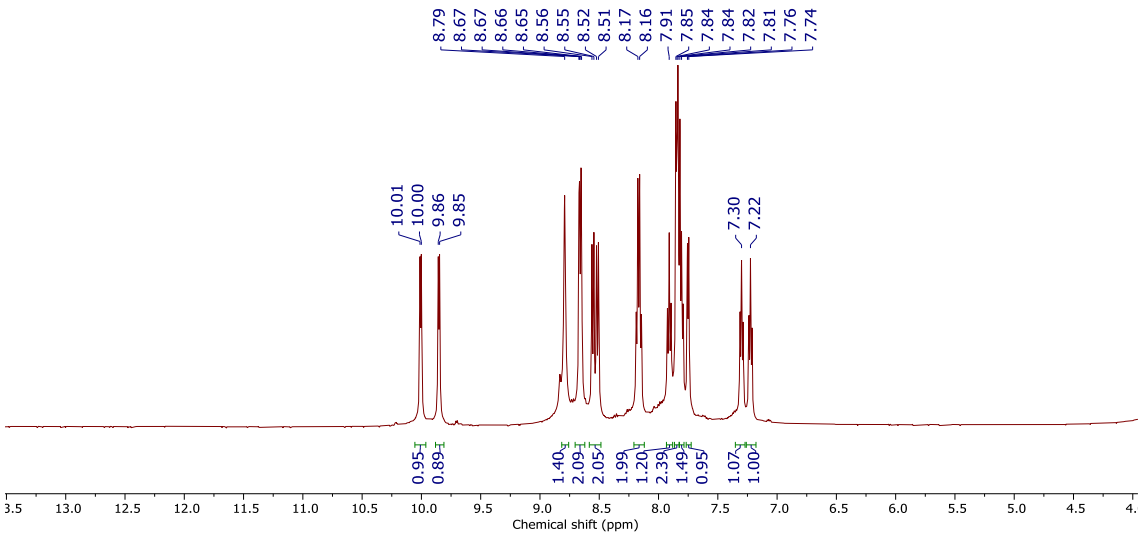

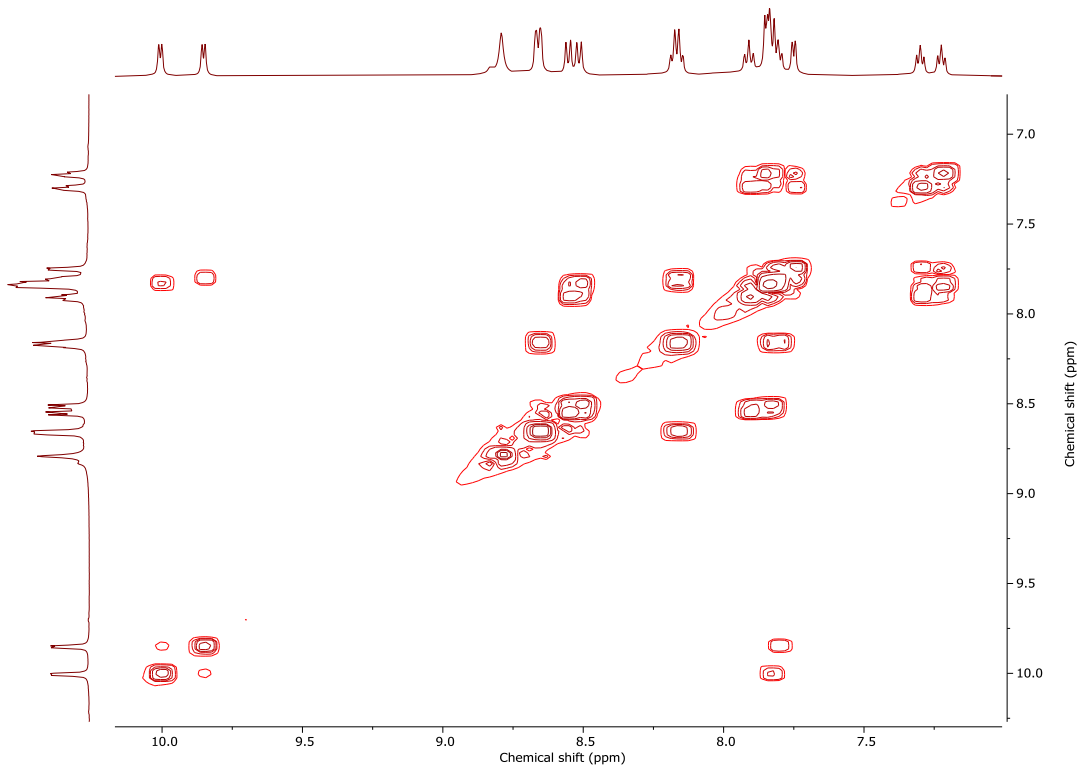

E) ^{1}H and COSY spectra for **Ru5**

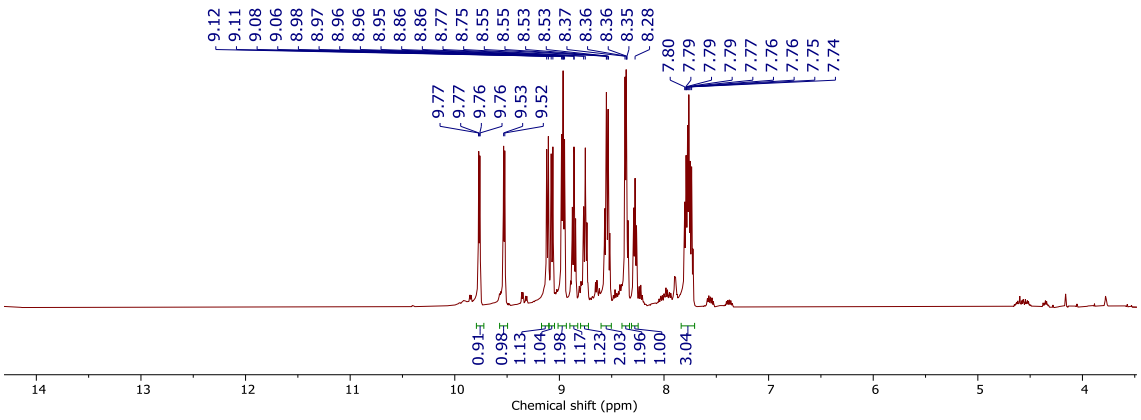

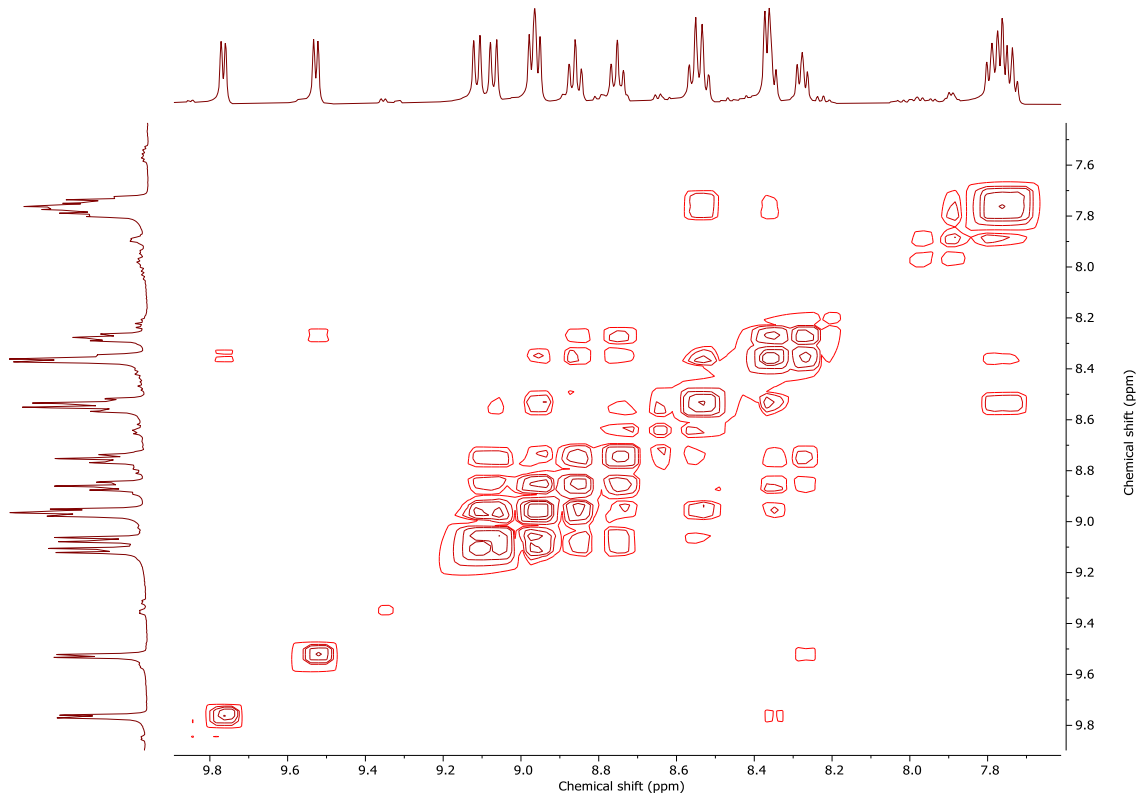

Figure S3. ESI-MS spectra for complexes **Ru1-5**

A) ESI-MS spectrum for **Ru1**

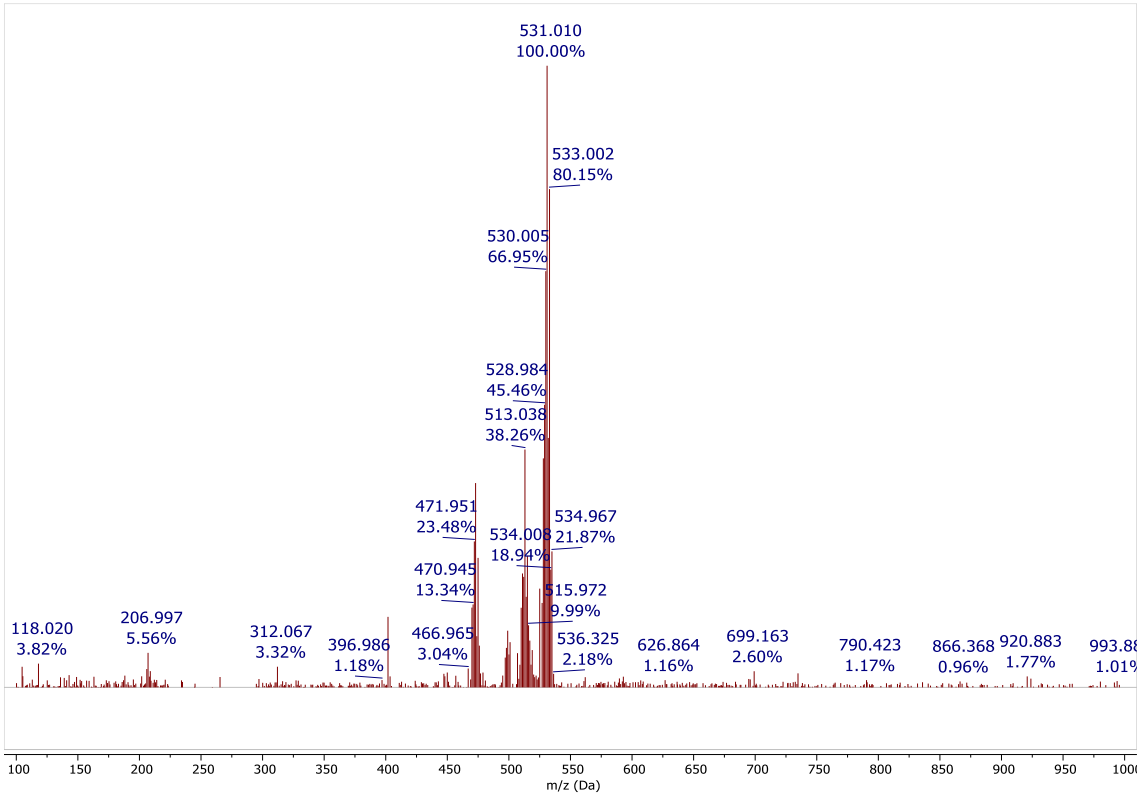

B) ESI-MS spectrum for **Ru2**

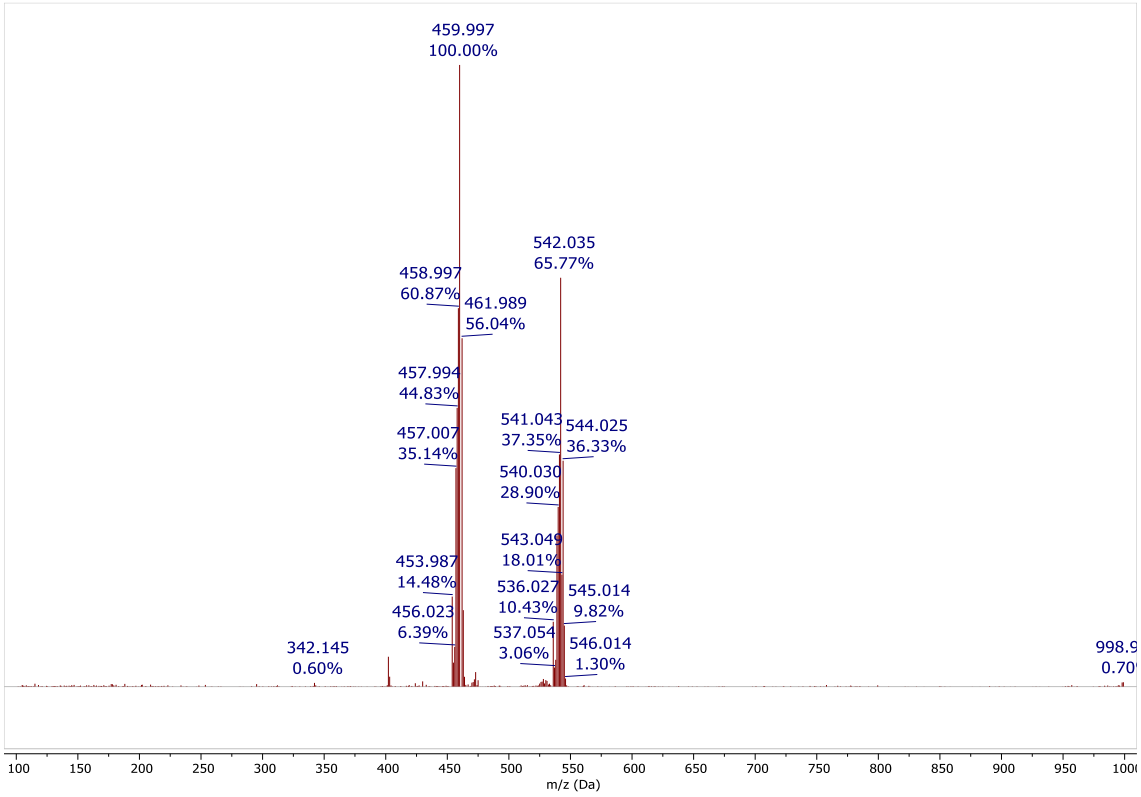

C) ESI-MS spectrum for **Ru3**

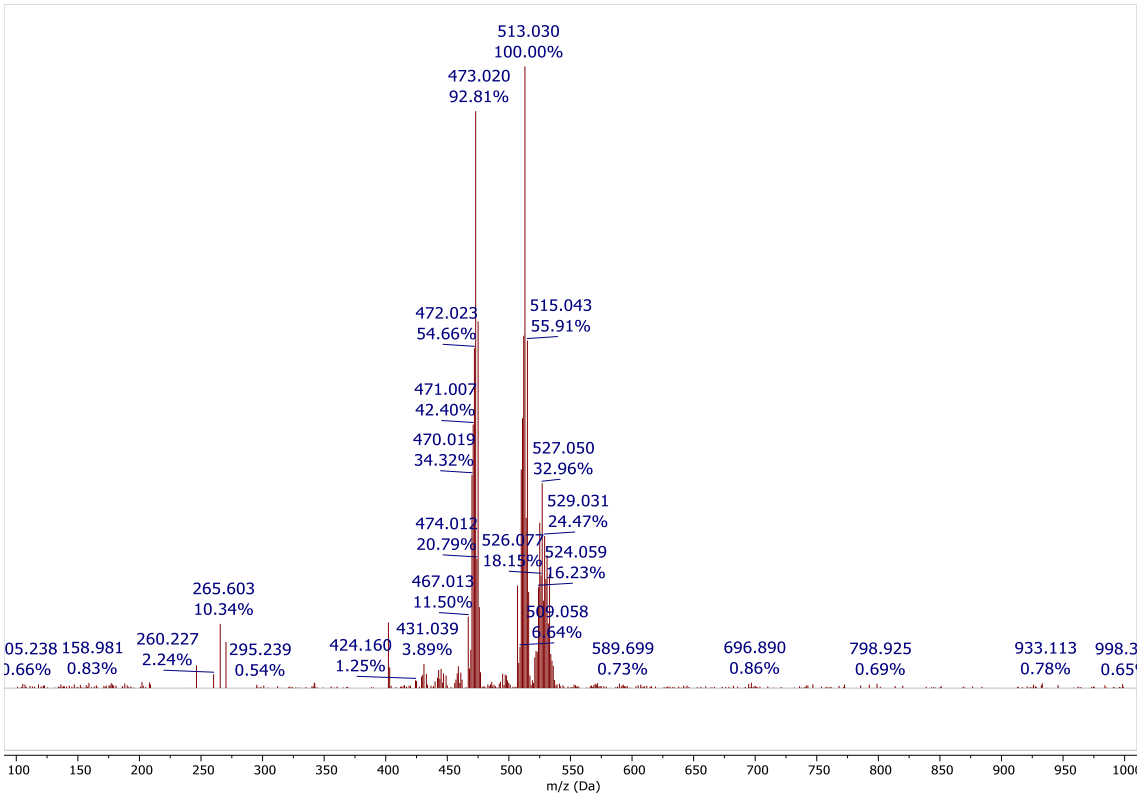

D) ESI-MS spectrum for **Ru4**

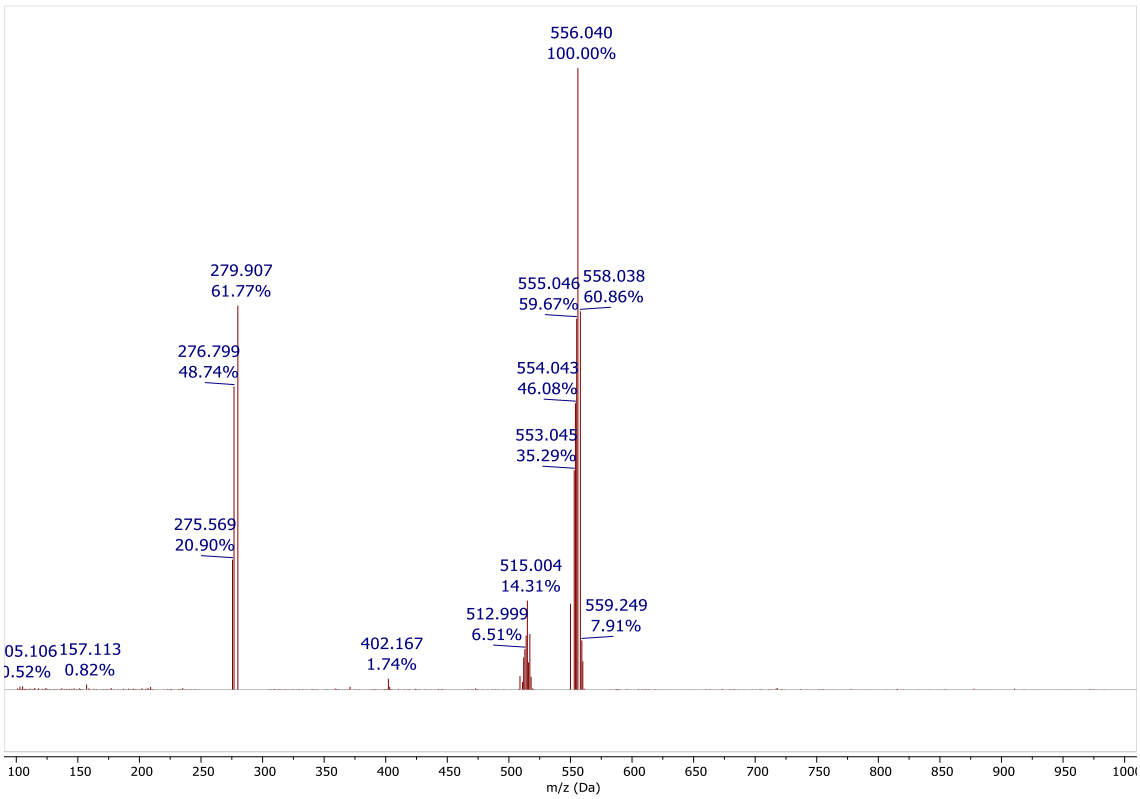

E) ESI-MS spectrum for **Ru5**

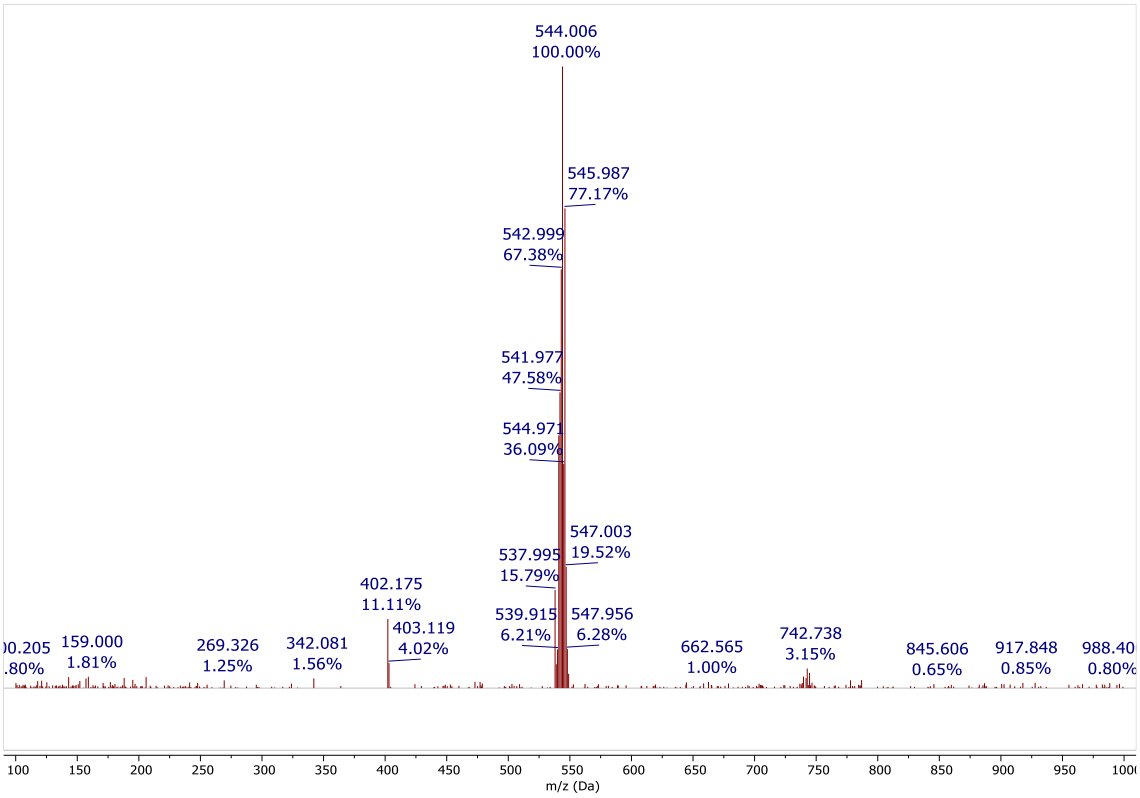

Figure S4. Vibrational spectroscopy in the infrared region data

A) Infrared spectrum for **Ru3**$(PF_6)_3$ in KBr pellet

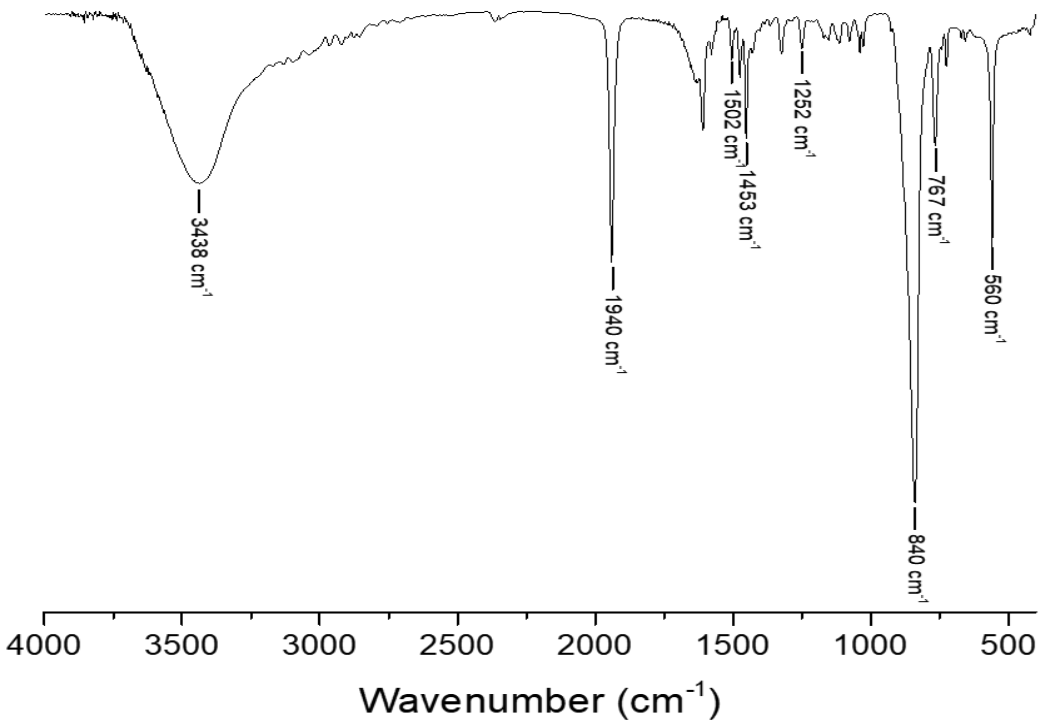

B) Infrared spectrum for **Ru5**$(PF_6)_3$ in KBr pellet

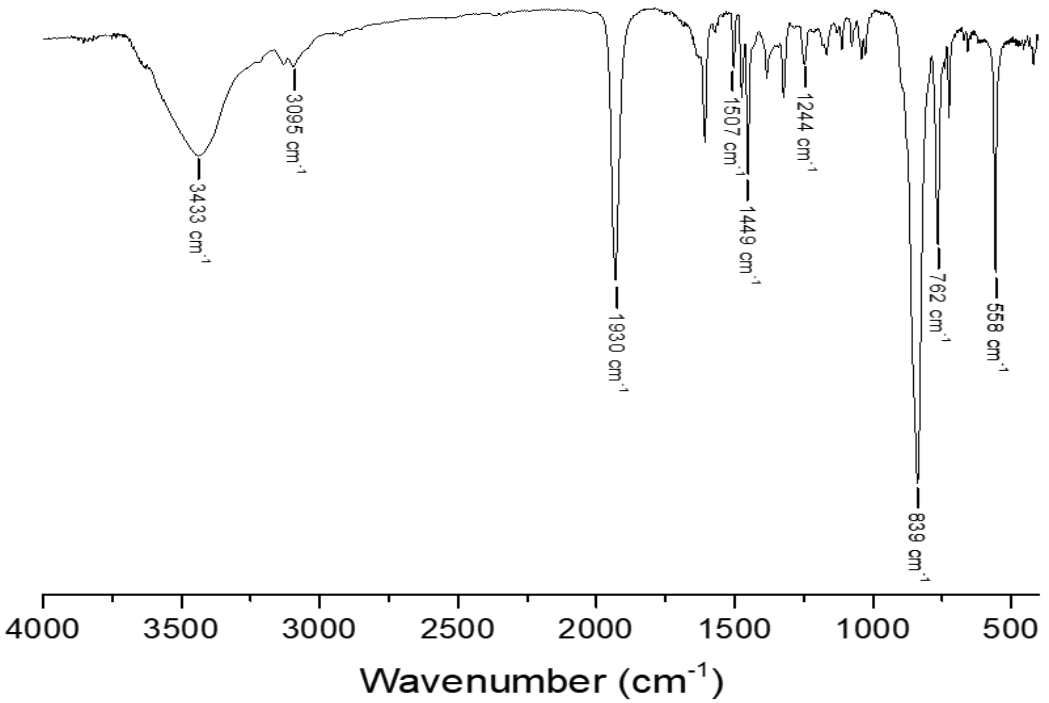

C) DFT-calculated infrared spectrum for **Ru3**

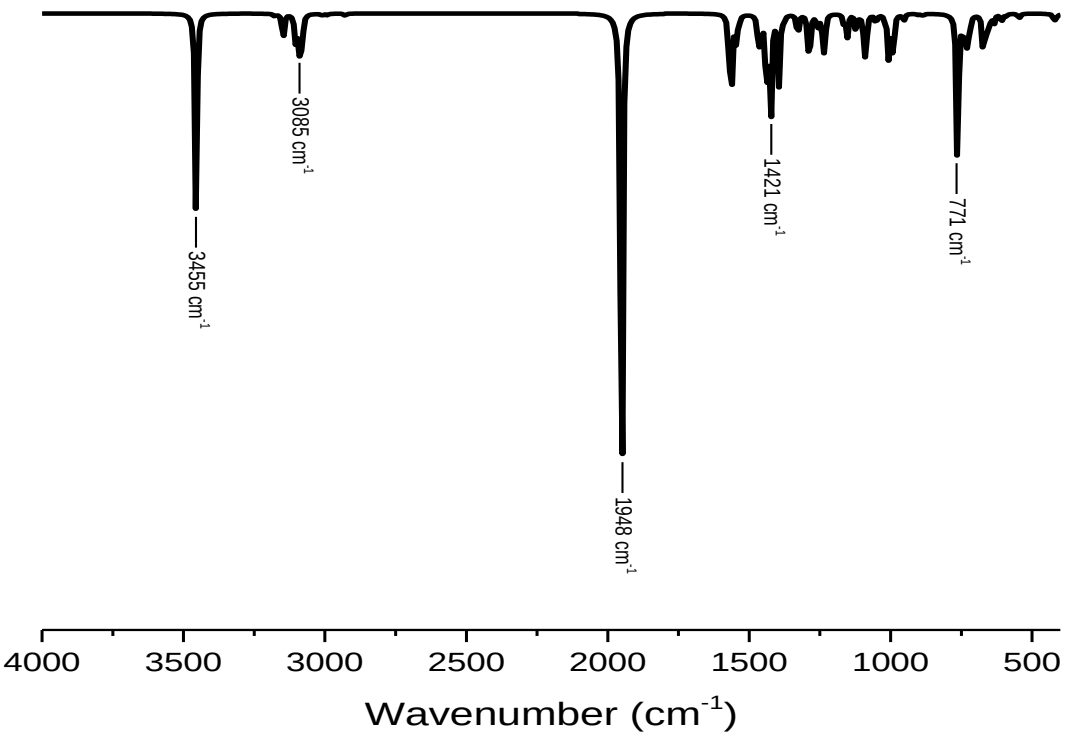

D) DFT-calculated infrared spectrum for **Ru5**

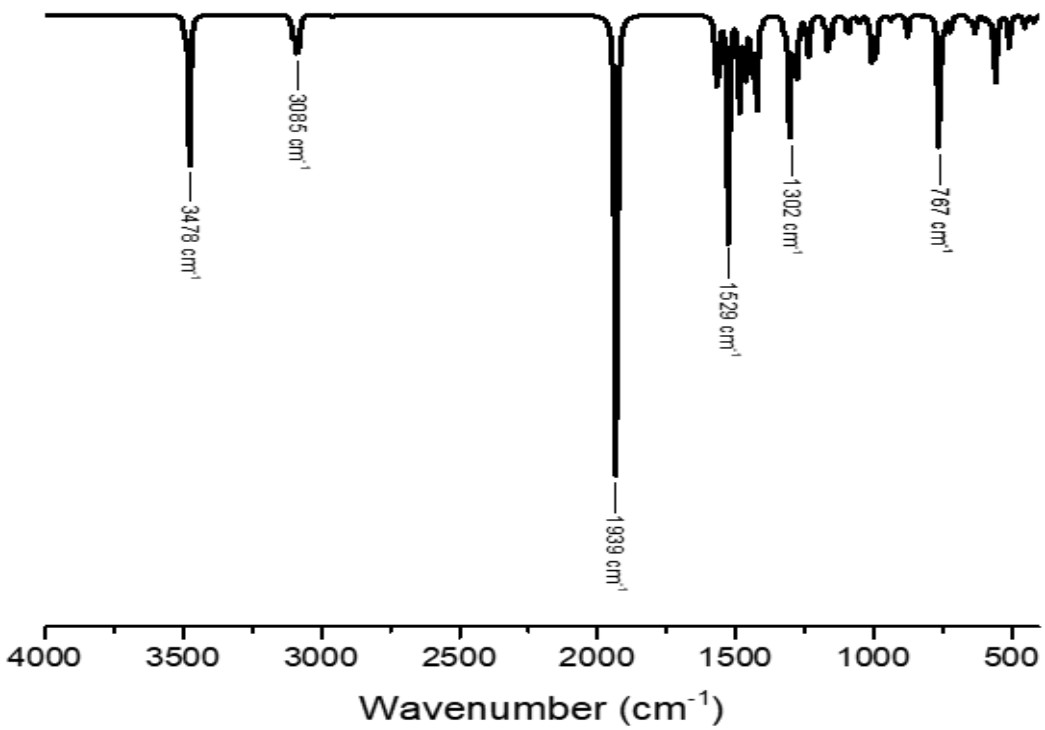

Figure S5. Cyclic voltammetry

A) Cyclic voltammograms for **Ru1** (left) and **Ru3** (right) in NaTFA 0.1 M pH 3.0.

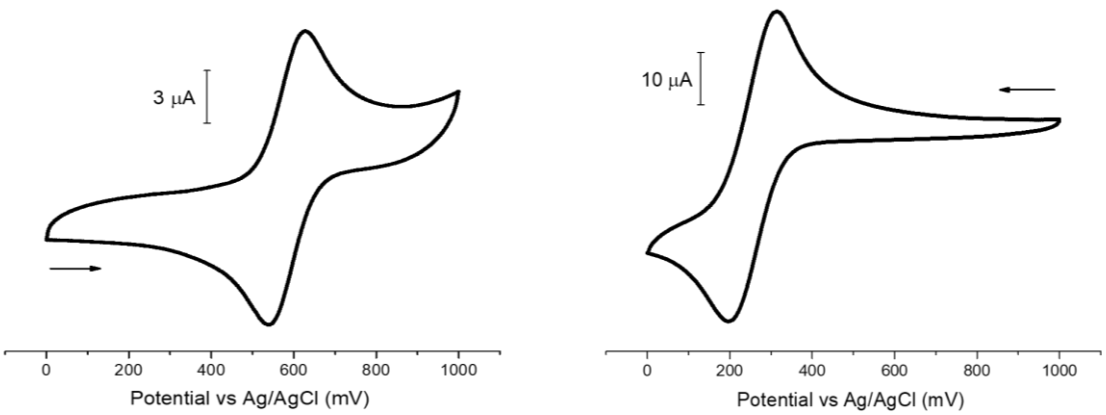

B) Cyclic voltammograms for **Ru4** (left) and **Ru5** (right) in NaTFA 0.1 M pH 3.0.

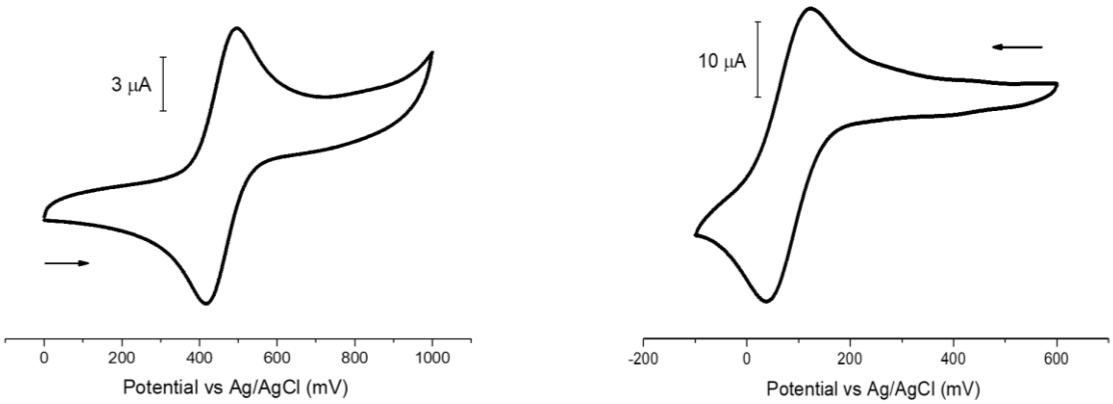

Figure S6. Experimental and simulated UV-vis spectra in acetonitrile solution (left) and orbital contributions (right) for **Ru1** (A) and **Ru3** (B).

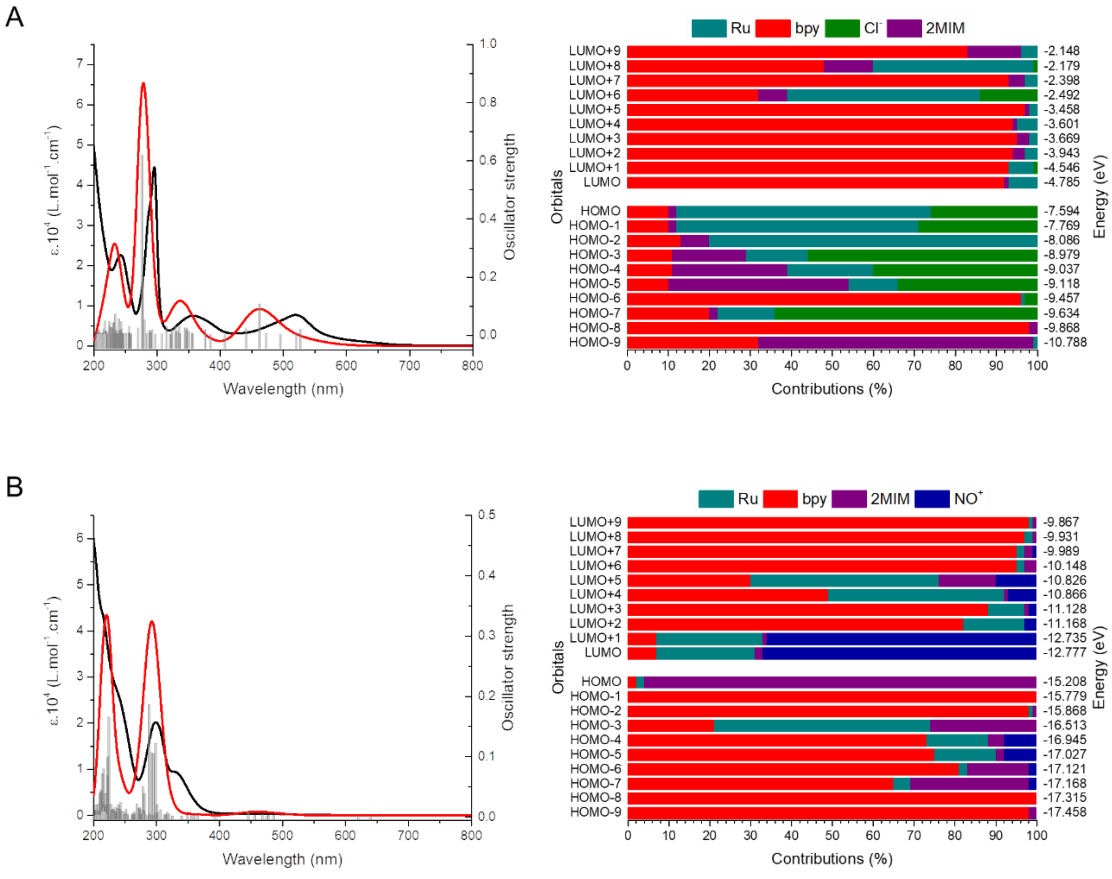

Figure S7. Experimental and simulated UV-vis spectra in acetonitrile solution (left) and orbital contributions (right) for **Ru4** (A) and **Ru5** (B).

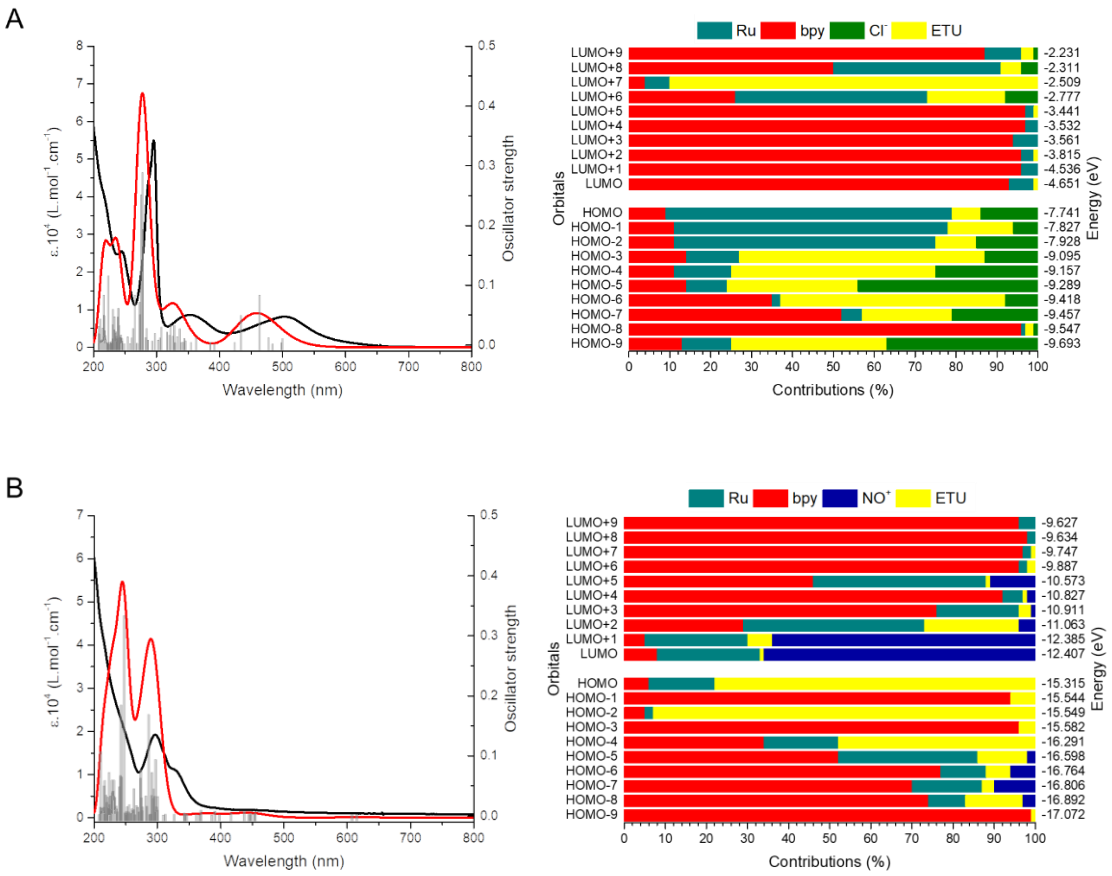

Figure S8. k^3-weighted, phase uncorrected, Fourier transform moduli (k range 2-14 Å^{-1}) of the experimental (circles) and best fit (solid line) EXAFS signals for complex **Ru2**. Inset: k^3-weighted EXAFS signals (circles) of complex **Ru2** and its corresponding best fits (solid line).

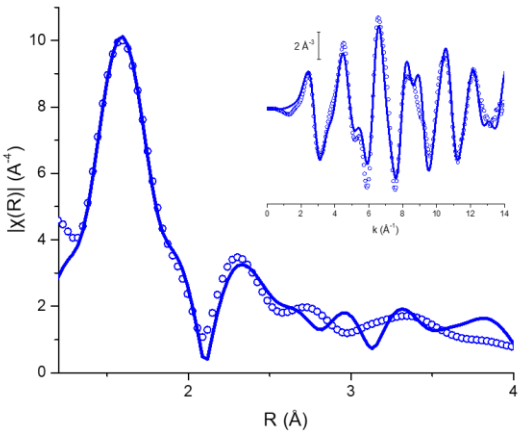

Table S1. Coordination number (CN), atomic distances (R), Debye-Waller factors (σ^2), fit parameters obtained from EXAFS refinement and respective DFT-simulated atomic distances (R_{DFT}) for complex **Ru2**

Parameters	**Ru2**			
	CN	R (Å)	R_{DFT} (Å)	σ^2 (Å^2)
Ru-N_{bpy}	4	2.04(3)	2.12(4)	0.0094
Ru-N_{2MIM}	1	2.10(5)	2.18(1)	0.0094
Ru-N_{NO_2}	1	2.10(5)	2.06(7)	0.0094
$S0^2$		0.859		
ΔE (eV)		0.32		
R-factor (%)		4.48		

Figure S9. Study of the equilibrium nitro-nitrosyl dependent on the pH, spectroscopic titration curves for complexes **Ru3** (A) and **Ru5** (B)

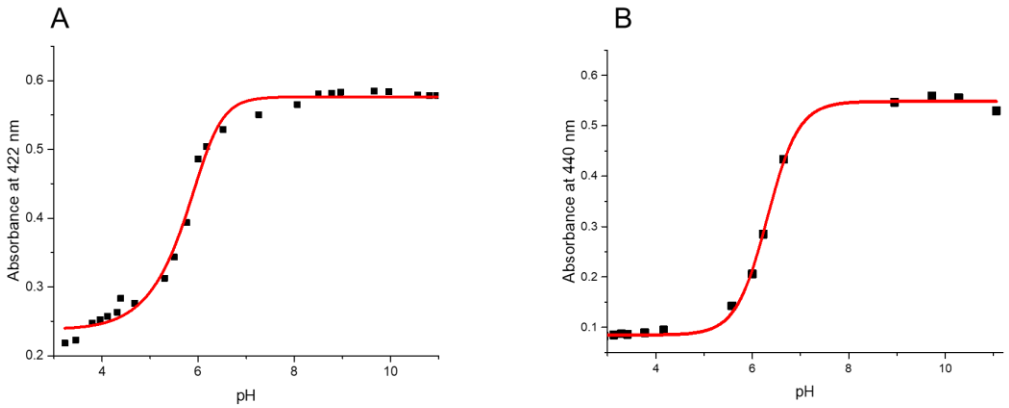

Figure S10. Investigation of NO and HNO. Spectroscopic profile and kinetic curves (insets) of NO/HNO detection from **Ru3** (A) and **Ru5** (B) after reduction with GSH, using cPTIO as probe.

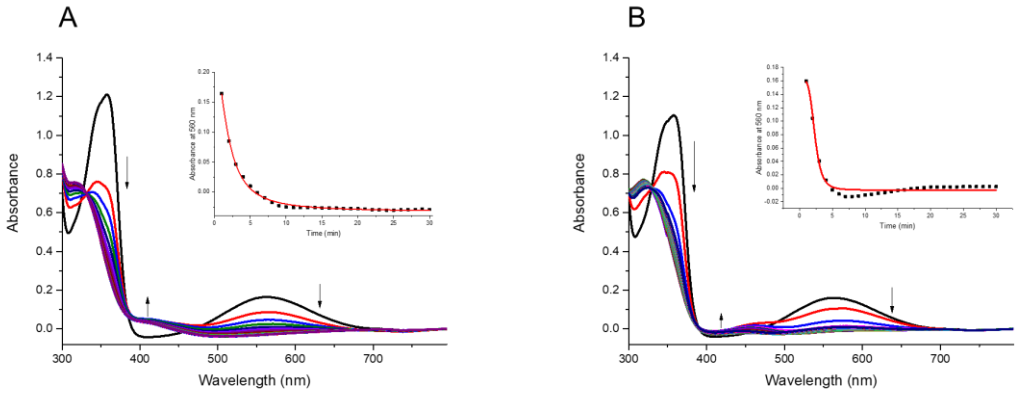

Figure S11. Investigation of NO and HNO using standard donors. UV-Vis absorption spectra for cPTIO reacting with DEA NONOate (A) and Angeli's salt (B). Black line is the initial spectrum and red is the last one.

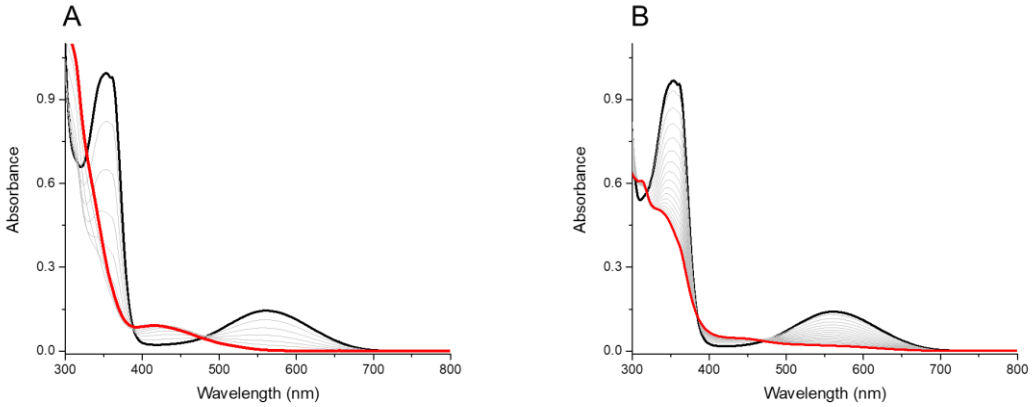

Figure S12. Investigation of NO and HNO production. (A) UV-vis absorption spectra of met-Mb in the presence of **Ru3** and glutathione (GSH). Inset: expansion of the Q bands region; (B) NO detection curves using the chemiluminescent sensor for the reaction of **Ru5** and GSH (black) and **Ru5** and GSH in the presence of ferricyanide (HCF, red).

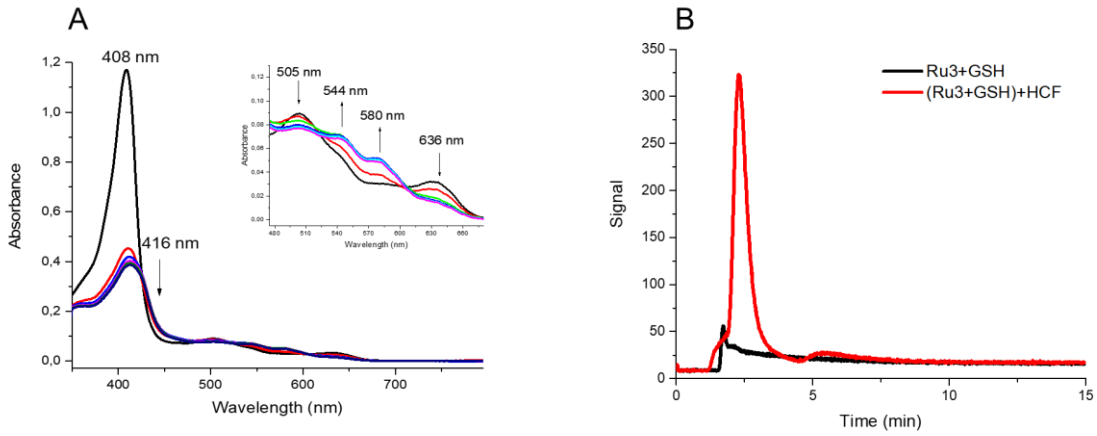

Table S2. Cell viability data (IC_{50} values) for complexes **Ru1-5** on human fibroblastic lung cells (MRC5 cell line). Results are expressed in µmol L^{-1}.

Ru1	Ru2	Ru3	Ru4	Ru5
61.44 ± 2.28	83.81 ± 3.99	147.29 ± 6.31	52.43 ± 1.54	112.95 ± 5.77

Figure S13. Dose-response curves for vasodilation assay in rat aorta using sodium nitroprusside (SNP, blue circles), the precursor *cis*-[$RuCl_2(bpy)_2$] (purple circles) and the organic ligands 2-methylimidazole (green squares) and ethylenethiourea (pink inverted triangles).

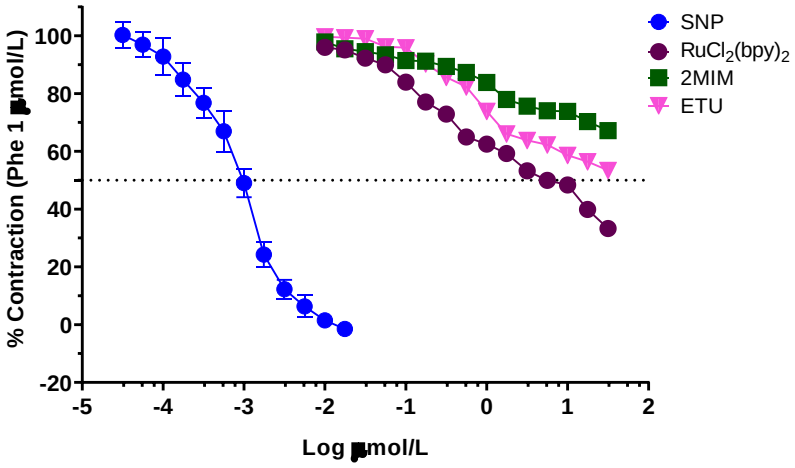

Table S3. IC_{50} values (µmol L^{-1}) for superoxide and hydroxyl radicals scavenger activities of the complexes determined by cytochrome c and TBARS methods, respectively.

Compound	IC_{50} – Cyt c/superoxide	IC_{50} – TBARS
Ru1	536.5 ± 11.2	55.1 ± 2.7
Ru2	> 1000	49.8 ± 3.8
Ru3	10.8 ± 0.4	34.1 ± 1.5
Ru4	459.4 ± 15.3	53.9 ± 0.9
Ru5	48.2 ± 1.9	33.2 ± 0.7

Figure S14.Chromatograms for tyrosine (A), 3-nitrotyrosine (B) and the mixtures of tyrosine, **Ru3** and superoxide (C); and tyrosine **Ru5** and superoxide (D).